Enhanced Mechanical Properties of Chitosan/EDTA-GO Nanocomposites Thin Films
(Peningkatan Sifat Mekanik Filem Nipis Nanokomposit Kitosan/EDTA-GO)

N.I. Syuhada, N.M. Huang*, S. Vijay kumar, H.N. Lim, S.A. Rahman, G.S.H. Thien,
N.A. Ibrahim, M. Ahmad & P. Moradihamedani

ABSTRACT

Nanocomposite thin films of chitosan/graphene oxide (CS/GO) and chitosan/ EDTA-GO (CS/EDTA-GO) were prepared by environmental friendly method and the properties were compared. The experimental results showed fine dispersion of GO and EDTA-GO in CS matrix and some interaction occur between the filler and the CS matrix that leads to better distribution of stress transfer. At 0.5 wt. %, both CS/GO and CS/EDTA-GO experienced maximum tensile stress by 51 and 71% compared with CS. Moreover, the elongation at break for both nanocomposites increases and the amount of filler increases.

Keywords: Chitosan; functionalized graphene oxide; graphene oxide; nancomposite thin films

ABSTRAK

Filem nipis nanokomposit kitosan/grafin oksida (CS/GO) dan kitosan/EDTA-GO (CS/EDTA-GO) telah disediakan dalam kaedah yang mesra alam dan sifat dibincangkan. Keputusan eksperimen menunjukkan GO dan EDTA-GO sangat larut di dalam matriks kitosan dan ini membantu dalam pemindahan tekanan. Pada pengisian 0.5 wt. %, kedua-dua CS/GO dan CS/EDTA-GO menunjukkan kadar kekuatan yang paling tinggi iaitu 51 dan 71% berbanding CS. Selain itu, pemanjangan filem bagi kedua-dua nanokomposit bertambah seiring dengan pertambahan pengisian.

Kata kunci: Filem nipis nanokomposit; grafin oksida; grafin oksida fungsian; kitosan

INTRODUCTION

Polymer nanocomposites present a radical alternative to conventionally- and macroscopically-filled polymers (Giannelis 1996). Polymer nanocomposites can be defined as polymers containing fillers that have one dimension smaller than 100 nm (Schadler et al. 2007). While traditional polymer composites require high loading of micrometre-sized filler (Schadler et al. 2007), polymer nanocomposites have been developed to have very low loading due to their nanometre-sized dispersion (Giannelis 1996). Compatibility between the nanofiller and the polymer matrix is the most significant factor, as it determines the dispersion and interface interactions that will influence the nanocomposite's macroscopic properties (Granick et al. 2003). There is a rapidly growing interest in the development of new multifunctional nanocomposites and attention is being channelled towards natural polymers for sustainable development and environmental preservation (Chabba et al. 2005).

Chitosan (CS) is a (β-1,4)-linked D-glucosamine derivative of the polysaccharide chitin and is the most abundant natural polysaccharide after cellulose (Layek et al. 2012). CS is inexpensive, renewable and has excellent biocompatibility. It has antibacterial properties and metal binding abilities and has widespread applications in sensors, medicine, metal chelating agents, adhesives, pharmaceuticals, food science, waste water treatment, biotechnology and textiles (Layek et al. 2012). However, the low mechanical properties and thermal stability of CS restrict its use in a wider range of applications (Tang et al. 2008).

Graphene is a flat monolayer of carbon atoms tightly packed into a two-dimensional (2D) lattice and is a basic building block for graphite materials of all dimensionalities (Fang et al. 2010). Over the past two decades, researchers have incorporated intercalated, exfoliated or expanded graphite platelets into polymers to produce nanocomposites (Mukhopadhyay & Gupta 2011). Carbon nanotubes are considered an ideal nanofiller in the polymer matrix; however, due to the expensive methods required to obtain carbon nanotubes, their application on an industrial scale is limited (Yang et al. 2010). Graphite, on the other hand, is easy to obtain and cheap, while graphene oxide (GO), which is the product of oxidising graphite, can be obtained using the Brodie, Staudenmaier and Hummers-Offemean methods (Hennig 1959; Hummers Jr & Offeman 1958).

The preparation of GO was carried out using the simplified Hummers method as described by (Chang et al. 2012). GO consists of functionalized graphene with oxygen-containing functional groups, bearing hydroxyl and epoxides on their basal planes, in addition to carbonyl and carboxyl groups located at the sheet edges (Morimune et al. 2012). The presence of these functional groups makes graphene oxide sheets strongly hydrophilic, allowing

graphene oxide to swell and disperse in water (Morimune et al. 2012), yielding colloidal suspensions of almost entirely individual graphene oxide sheets (Dikin et al. 2007).

GO exhibits large surface area and the functional groups may provide a platform for further modifications and attachments with other organic or non-organic compounds. It can be chemically functionalised, dispersed in polymer matrices and deoxygenated to yield novel composites (Stankovich et al. 2006). The unique surface properties, large surface area, layered structure and easy exfoliation into monolayers under water means that graphene oxide is a suitable building block for fabricating versatile functional materials via covalent or non-covalent approaches (Veerapandian et al. 2012). Both covalent and non-covalent functionalization of GO has been reported to generate stable dispersions of chemically modified graphene (CMG) platelets in organic solvents and also to enhance their compatibility with various polymer matrices (Potts et al. 2011).

EDTA-GO was prepared by covalent functionalization of the hydroxyl groups of GO as described by Hou et al. 2010; Vijay Kumar et al. 2012. The outline of the synthesis is presented in Figure 1 and it was observed that EDTA-GO is able to disperse well in water due to the hydrophilic properties of EDTA. Both nanocomposites were produced by non-covalent dispersion method that involve the mixing and stirring of filler (GO and EDTA-GO) into the chitosan matrix. This environmental friendly and cost effective procedure is able to produce polymer nanocomposites thin films in large scale.

MATERIALS AND METHODS

MATERIALS

Graphite flakes (3061, Asbury Graphite Mill Inc.), potassium permanganate (KMnO$_4$) (98%) and sodium hydroxide (NaOH) were purchased from Merck (Whitehouse Station, New Jersey). N-(trimethoxysilylpropyl) ethylenediamine triacetic acid sodium salt (silane-EDTA) aqueous solution (45%) was purchased from Gelest Inc. (PA, USA). Sulphuric acid (HCl) and hydrogen peroxide (H$_2$O$_2$, 30%) were purchased from Systerm (Kuala Lumpur, Malaysia). Chitosan with low molecular weight (Mw=100,000–300,000) was obtained from Acros Organics (New Jersey, USA). All other reagents and chemicals were of analytical grade and used as received. Deionised water (DIW) was used during sample preparation.

PREPARATION OF EDTA-GO

Graphene oxide (GO) was prepared using the simplified Hummers method (Chang et al. 2012; Vijay Kumar et al. 2012) and GO surface via silylation EDTA was carried out as reported (Hou et al. 2010; Vijay Kumar et al. 2012) and the illustration of the procedure followed Scheme 1. 300 mL of ethanol was poured into a three-neck round flask. About 200 mg of dried GO was added to the ethanol solution

and treated with ultrasonication for 1 hr. 1.25 g of TETA in 17 mL of DIW was added drop wise into the flask under vigorous stirring. The flask was then placed in an oil bath and heated at 65°C for 12–16 h. The product was cooled to room temperature over 30 min. The final product was washed and centrifuged with a mixture of 200 mL acetone and 80 mL DIW and later dried at 80°C for 12 h.

THIN FILMS PREPARATION

The preparation of CS/GO and CS/EDTA-GO nanocomposites thin films were carried out using a simple solution mixing method. About 1000 mg of chitosan was dissolved in 30 mL aqueous acetic acid solution and designated loading amounts of GO and EDTA-GO (0.05, 0.5 and 1 wt. %) were dissolved in 20 mL of DIW. The solutions were then treated with mild sonication for 9 h. Homogenous solutions of GO and EDTA-GO in DIW were observed. Each of the solutions was poured into several chitosan solutions and subjected to vigorous stirring for 48 h. Each of the final solutions was then poured into two petri dishes, with 20 mL of solution in each, and dried under the fumehood for 6 days. The final products were flexible, free-standing thin films.

CHARACTERIZATION

X-ray diffraction measurements were carried out using a Siemens D5000 X-Ray diffractrometer with Cu Kα X-ray source radiation (λ=1.5418 Å and scan rate of 0.02°/s). UV–visible spectroscopy was undertaken using a Thermo Scientific Evolution 300 UV–vis Spectrometer over the range of 200–800 nm. Glass transition temperatures of the nanocomposite thin films were investigated using a Netzsch DSC 200 F3 calorimeter. The heating temperature was ramped from room temperature up to 250°C at a rate of 20°C/min, while the gas flow rate was fixed at 20 mL/min. The mechanical strength of the film was tested using a Shimadzu Autograph AG-X universal tester. The test was conducted at room temperature and the extension rate was fixed at 5 mm/min. The nanocomposite films used were rectangular, with dimensions of 60×10 mm^2. The gauge length for all nanocomposite films was fixed at 40 mm. Field emission scanning electron microscopy (FESEM) measurements were taken using a JEOL JSM-6700F microscope.

EXPERIMENTAL RESULTS

Chitosan is soluble in a water/acetic acid medium and has many hydroxyl and amino groups available for interaction (Layek et al. 2012). After reaction with the filler, it was observed that the colour of the nanocomposites changes as the weight percentage of the filler increase. As more amount of GO was added to the CS solution, the colour of the nancomposites changed from clear solution to dark brown. Similar changes occurred on CS/EDTA-GO nanocomposites whereby the clear solution seems to get darker as the amount of EDTA-GO is increased. The change of colour in CS/EDTA-GO was due to the restoration of the conjugation
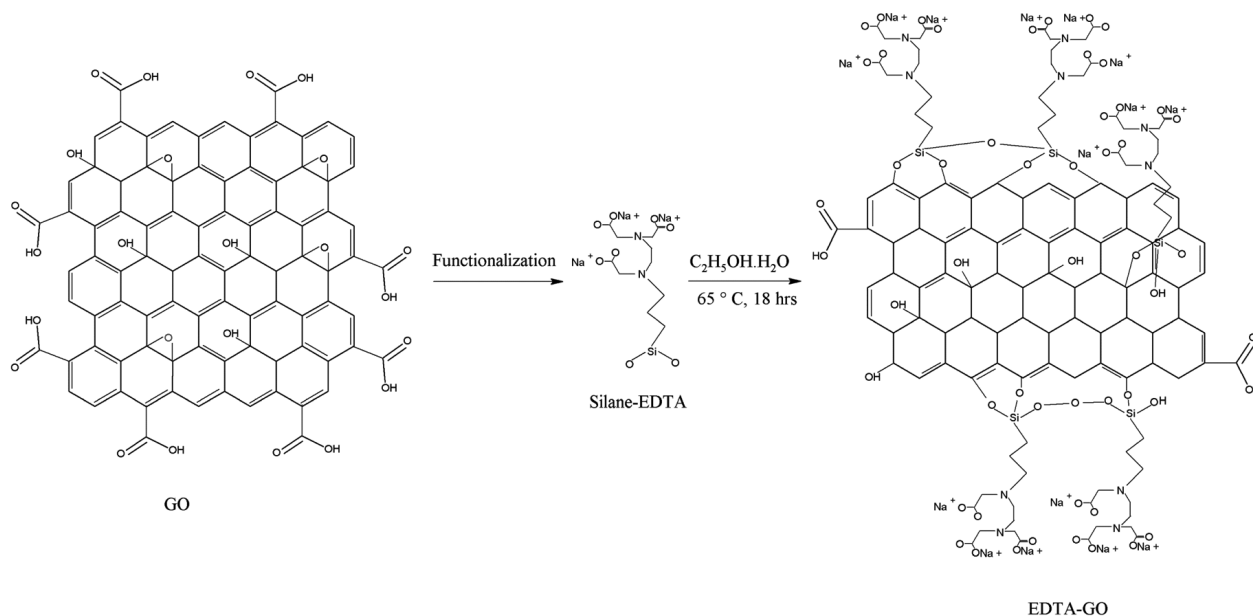
FIGURE 1. Outline synthesis of EDTA-GO. Silane-EDTA molecules are attached on the surface of GO via silylation

groups (Hou et al. 2010). Figure 2 showed the photograph of the nanocomposites and their respective thin films. As seen in the picture, stable and homogenous dispersion of the nanocomposites were observed and their respective thin films were smooth and flexible.

X-RAY DIFFRACTION (XRD)

X-Ray Diffraction of CS, GO and EDTA-GO are shown in Figure 3(A). Raw graphite exhibits an intense peak at 26.5° with an interlayer d-spacing of 0.34 nm and can be assigned to the (002) facet of hexagonal crystalline graphite (Szabó et al. 2005; Wang et al. 2008). After the graphite undergoes the oxidation process, a characteristic peak of graphene oxide is observed at 10.2° with d-spacing of 0.88 nm. The increase in d-spacing indicates larger interlayer spacing due to the intercalating oxygen functional groups (Shen et al. 2012). After functionalization, EDTA-GO exhibits a broad peak at 13.0° with d-spacing of 0.68 nm. This peak is almost non-existent, demonstrating the attachments of new functional groups throughout the surface of GO.

XRD patterns of the nanocomposites are displayed in Figure 3(b) and 3(c). The characteristic peaks of CS at 10.0° and 20.0° correspond to crystal (1) and crystal (2) in chitosan (Wang et al. 2005). Crystal (1) corresponds to the hydrated crystalline structure, whereas crystal (2) corresponds to the relatively crystalline lattice (110) of chitosan (Rhim et al. 2006). After incorporation of GO and EDTA-GO, new broad peak was observed and shifted at around 25°. The broadening of the peak is most likely due to the decreased in CS crystallinity and disordered exfoliated structure. After mixing, GO and EDTA-GO may experience fully exfoliation in CS polymer matrix. Works on chitosan/nanoclay showed a similar broadening suggesting that the crystalline degree of chitosan decreases as more amount of filler is used.
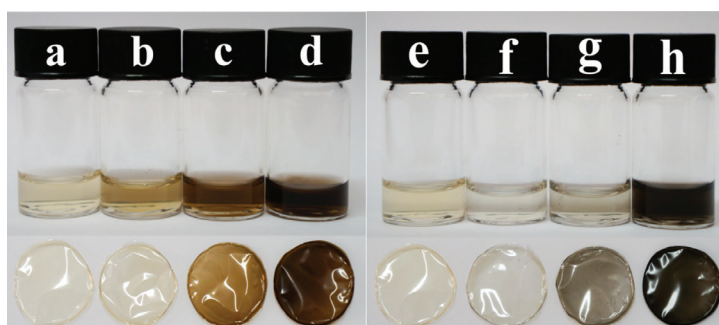

FIGURE 2. Photographs of the nanocomposites solution and their respective films with increasing amount of filler. (a, e) CS, (b) CS/ 0.05 wt% GO, (c) CS/ 0.5 wt% GO, (d) CS/ 1.0 wt% GO, (f) CS/ 0.05 wt% EDTA-GO, (g) CS/ 0.5 wt% EDTA-GO and (h) CS/ 1.0 wt% EDTA-GO. All the nanocomposites solutions are in good dispersion and the thin films are smooth and flexible
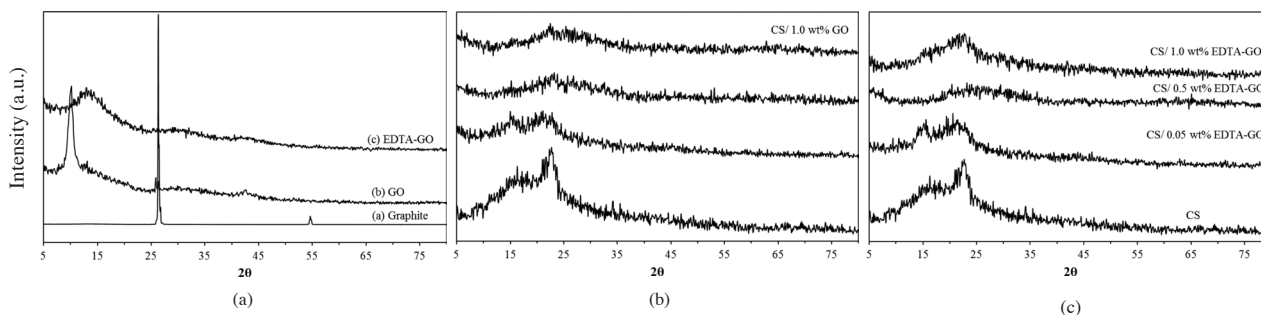
FIGURE 3. (a) XRD patterns of graphite, GO and EDTA-GO, displayed the XRD patterns of
(b) CS/GO and (c) CS/EDTA-GO nanocomposites

UV-VISIBLE SPECTROSCOPY

The dispersion uniformity of the nanocomposites was characterised by UV-vis transmittance measurement between 200 and 800 nm. Figure 4 shows the variation of the UV-vis transmittance for (a) CS/GO and (b) CS/EDTA-GO. The distribution of GO and EDTA-GO in CS solution strongly depends on how well they can disperse in water. GO can disperse well in CS solution due to the existence of oxygen functional groups on GO sheets (Pan et al. 2011). As for CS/EDTA-GO, the as prepared EDTA-GO is very hydrophilic and is a highly water-soluble compound that is able to produce good dispersion in CS matrix. From the result, it was observed that the li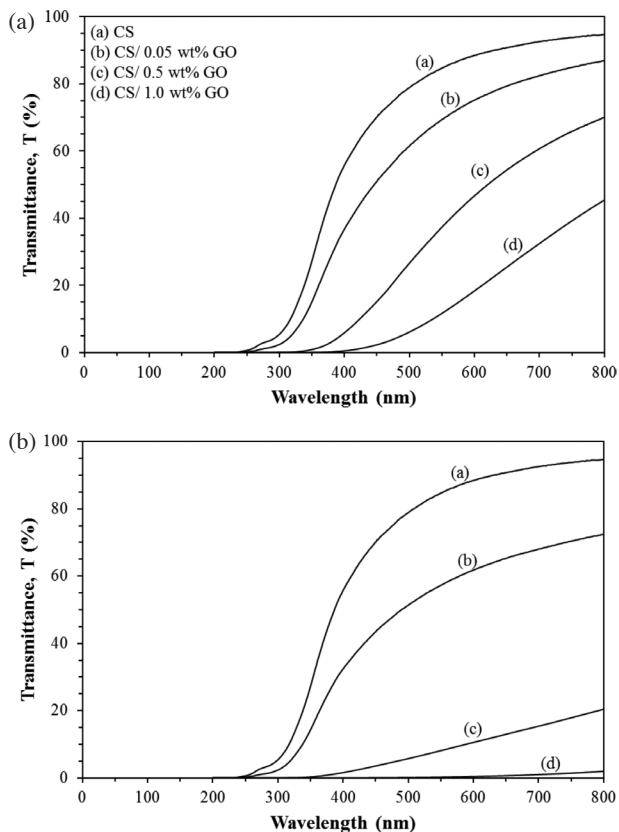ght transmittance of the nanocomposites decreases as the amount of filler is increases. For pure CS, the light transmittance at 800 nm was 95% and decreased to 45% at CS/1.0 wt. % GO. The light transmittance decreased to 2% at CS/1.0 wt. % EDTA-GO at the same wavelength. CS/GO nanocomposites still maintain favourable light transmittance whereas CS/EDTA-GO was quite poor in light transmittance. Measurement at different locations on the thin films for both nanocomposites showed similar light transmittance, suggesting uniform dispersion of the material for both nanocomposites (Pan et al. 2011).

GLASS TRANSITION TEMPERATURE (T_g)

The usage of carbon materials as filler into polymer matrix may change the thermal or the mechanical characteristics of the nanocomposites. In general, the important factor would be the interface region between the filler and the polymer. Interface region refers to the interaction of the polymer chains with the surface of the particle which can alter the chain kinetic in the region surrounding the particle (Ash et al. 2002). Glass transition temperature (T_g) was used to examine the thermal behaviour of the nanocomposites. The T_g of chitosan is difficult to pursue due to the difficulty in sample preparation and the hydroscopicity of the samples (Rana et al. 2010). Numerous works on the search of the T_g of CS have been done with different techniques. Dong et al. measured the T_g of chitosan by using four different techniques and the range of the T_g is between 140 and 150°C (Dong et al. 2004) and Cervera et al. (2014) found that the T_g of chitosan to be around 130-139°C.

Several factors may affect the difference in Tg such as the interaction between the polymer chains, ionic or hydrogen bonding between the composites. In this research, the T_g of CS was found around 120°C. T_g of the nanocomposites is displayed in Figure 5 where 'x' represents the amount of filler. Significant increase in T_g has been observed for both nanocomposites. Highest T_g for CS/GO nanocomposites was observed at 1 wt. % (137.2°C), while 0.05 and 0.5 wt.% bearing the T_g at 128.9 and 135.1°C. Overall, CS/ 1.0 wt% EDTA-GO has the highest T_g at 146.7°C while 0.05 and 0.5 wt. % bearing the T_g at 135.0 and 141.4°C. It is clear indication that, strong interaction occurred between the filler and CS –through hydrogen bonding (that will be discussed in the next section) that
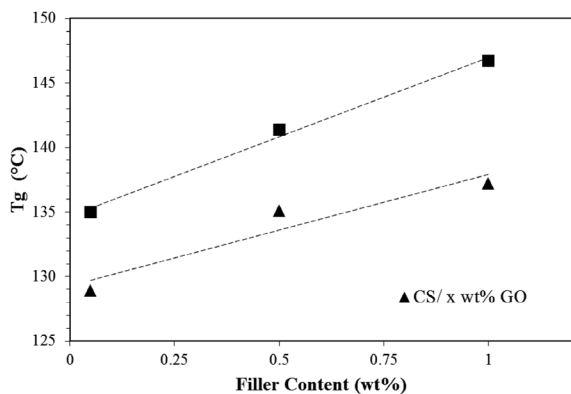

FIGURE 4. UV-Visible spectra of (a) CS/GO and
(b) CS/EDTA-GO nanocomposites

FIGURE 5. Glass-transition temperature (T_g) of the nanocomposites

increases the T_g of CS. From UV-visibile spectroscopy analysis, in a well-dispersed condition, the amount of filler would provide interfacial area which the bulk properties of the polymer can be altered. Thus, restricting its chain mobility and increase its T_g.

MECHANICAL PROPERTIES ANALYSES

There are several parameters that affect directly the mechanical properties of a material such as the properties of the filler and the polymer matrix, filler volume fraction, the interfacial region and filler shape. The most important parameter would be the compatibility and the bonding between the filler and the polymer matrix. The type of bonding varies from strong chemical bonds or weak Van der Waals.

Typical stress-strain curves of chitosan and its nanocomposites are shown in Figure 6 and summarized in Table 1. From the figure, the tensile stress at break increased and exceeded pure CS for both nanocomposites. This is a clear indication that the addition of GO and EDTA-GO significantly improved the tensile properties of CS. Maximum tensile stress of CS/GO nanocomposites was observed at 0.5 wt. % with an increment at about 51%. The maximum tensile stress was observed at CS/ 0.5 wt. % EDTA-GO, with increment of 71%.

The enhanced tensile stress of the nanocomposites may be due to two important factors: Dispersion level of GO and EDTA-GO in CS matrix and the strong interaction between them. It is very crucial to have uniform dispersion between the filler and the CS matrix as this will provide the interfacial region between them. GO has many hydrophilic functional groups such as –COOH and –OH. Additionally, the surface of GO sheets are negatively charged when dispersed in water, apparently as a result of ionization of carboxylic acid and phenolic hydroxyl groups on the GO sheets (Li et al. 2008) that may induces better dispersion of GO at the individual sheet level in
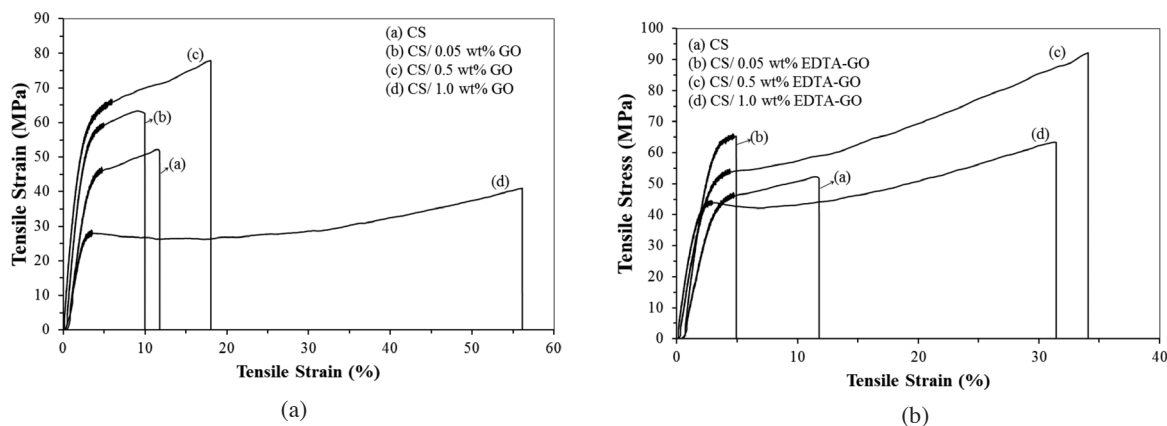

(a)

(b)

FIGURE 6. Stress-strain curves of (a) CS/GO and (b) CS/EDTA-GO nanocomposites

TABLE 1. Mechanical properties of CS and its nanocomposites

Sample	Tensile Strength, σ_y MPa	Elongation at Break, ϵ_b %
Pure CS	54.95	11.59
CS/ 0.05 wt% GO	65.36	9.12
CS/ 0.5 wt% GO	82.82	18.04
CS/ 1.0 wt% GO	39.12	40.69
CS/ 0.05 wt% EDTA-GO	68.08	4.64
CS/ 0.5 wt% EDTA-GO	94.11	34.08
CS/ 1.0 wt% EDTA-GO	64.01	31.32

water. CS is very hydrophilic biopolymer and exhibits polycationic properties. It has many –NH$_2$ and –OH that can be protonated to polycationic material as we mix with acetic acid. Inter-molecular hydrogen bonding can happen between these functional groups and may induce very fine codispersion in the molecular scale (as illustrated in Scheme 1).

In case of CS/EDTA-GO, the introduction of hydrophilic EDTA groups improved its compability in water and generated stable solution. Since EDTA-GO has more –COOH and –OH groups throughout the sheets and more inter-molecular hydrogen bonding are expected, resulting in very fine codispersion in the molecular scale (as illustrated in Scheme 2). Thus, improving the strength of CS films and even exceeded the tensile stress of CS/GO nanocomposites. It is interesting that the nanocomposites have not only higher tensile stress but also larger elongation at break compared to CS. The elongation at the break point of the film with 1 wt. % GO increased about 251% in comparison of CS. As for CS/ 1.0 wt. % EDTA-GO, it increased about 170%. Both nanocomposites experienced decrease in tensile stress at 1.0 wt%. This pattern is believed due to plasticizer effect. Although the mechanism of the plasticization is unclear and several theories have been proposed but the effect of plasticization is recognizable;

decrease in stress and increase in strain. However, additional work is needed to investigate it.

FESEM was employed to observe the cross-section of fractured films, and the image is shown in Figure 7. Cross-sections of the nanocomposite films are very different from those of CS. The nanocomposite films show stacks of sheets, which shows that neither nanocomposite loses its graphene-like properties (Pan et al. 2011). Overall, it is crucial that the nanocomposites exhibit good dispersion to begin with as it is a determining factor for preparing reinforcing nanocomposites. As discussed above, as GO has many oxygen-containing groups on its surface, hydrogen bonding may occur with the amine and the hydroxyl groups of CS. EDTA-GO however, have many carboxyl and hydroxyl groups throughout its surfaces and give rise to more probable hydrogen bonding. Compiling these factors and in addition to the remarkable properties of graphene-based filler, this can significantly improve the mechanical properties of the nanocomposites.

CONCLUSION

Nanocomposites of CS/GO and CS/EDTA were prepared by environmental friendly method. Both nanocomposites showed remarkable dispersion at molecular level. At 0.5
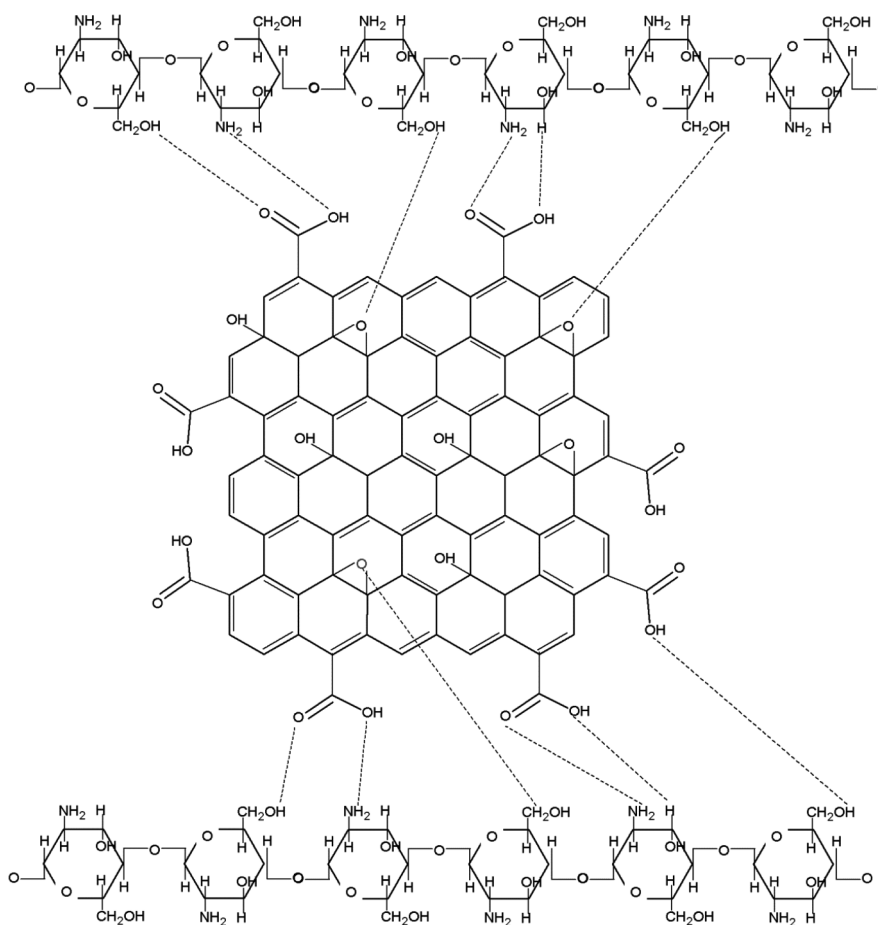
SCHEME 1. Illustration of the interaction between CS and GO. The amine and hydroxyl groups of CS are able to form hydrogen bonding with the carboxyl and hydroxyl groups of GO
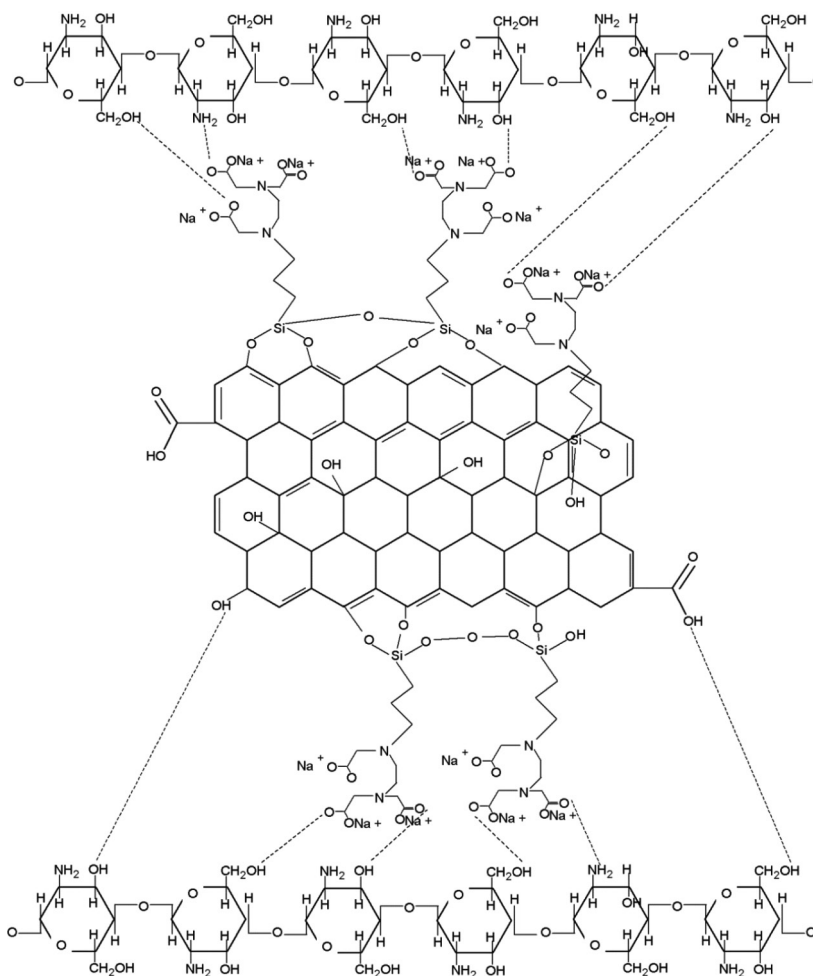
SCHEME 2. Illustration of the interaction between CS and EDTA-GO. Introduction of hydrophilic EDTA groups has improved its dispersion in the nanocomposites and since EDTA-GO has more carboxyl and hydroxyl groups attached throughout its surface, more intermolecular hydrogen bonding are expected with the amine and hydroxyl groups of CS
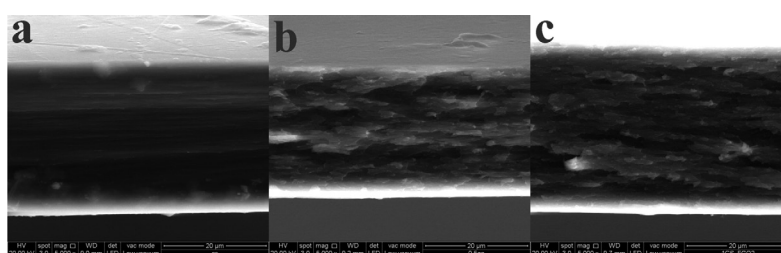

FIGURE 7. FESEM images on the cross-section of the thin films after fractured (a) CS, (b) CS/GO and (c) CS/EDTA-GO

wt. %, both CS/GO and CS/EDTA-GO experienced maximum tensile stress by 51 and 71% compared to CS. Additionally, the elongation at break increases as the amount of filler is increases. To the best of our knowledge, this is the first study of the mechanical properties of CS/EDTA-GO. Our work demonstrated simple and yet cost effective method to produce improved mechanical properties of the nanocomposites thin films in a large scale that may find more important applications such as biomedical and sensors.

REFERENCES

Ash, B.J., Schadler, L.S. & Siegel, R.W. 2002. Glass transition behavior of alumina/polymethylmethacrylate nanocomposites. *Materials Letters* 55(1): 83-87.

Cervera, M., Fernández, J., Heinämäki, M., Räsänen, S.L., Maunu, M., Karjalainen, O.M., Acosta, A., Iraizoz, C. & Yliruusi, J. 2004. Solid-state characterization of chitosans derived from lobster chitin. *Carbohydrate Polymers* 58(4): 401-408.

Chabba, S., Matthews, G.F. & Netravali, A.N. 2005. 'Green'composites using cross-linked soy flour and flax yarns. *Green Chem.* 7(8): 576-581.

Chang, B.Y.S., Huang, N.M., An'amt, M.N., Marlinda, A.R., Norazriena, Y., Muhamad, M.R., Harrison, I., Lim, H.N. & Chia, C.H. 2012. Facile hydrothermal preparation of titanium dioxide decorated reduced graphene oxide nanocomposite. *International Journal of Nanomedicine* 7: 3379.

Dikin, D.A., Stankovich, S., Zimney, E.J., Piner, R.D., Dommett, G.H.B., Evmenenko, G., Nguyen, S.B.T. & Ruoff, R.S. 2007. Preparation and characterization of graphene oxide paper. *Nature* 448(7152): 457-460.

Dong, Yanming, Yonghong Ruan, Huiwu Wang, Yaging Zhao & Danxia Bi. 2004. Studies on glass transition temperature of chitosan with four techniques. *Journal of Applied Polymer Science* 93(4): 1553-1558.

Fang, M., Long, J., Zhao, W., Wang, L. & Chen, G. 2010. pH-responsive chitosan-mediated graphene dispersions. *Langmuir* 26(22): 16771-16774.

Giannelis, E.P. 1996. Polymer layered silicate nanocomposites. *Advanced Materials* 8(1): 29-35.

Granick, S., Kumar, S.K., Amis, E.J., Antonietti, M., Balazs, A.C., Chakraborty, A.K., Grest, G.S., Hawker, C., Janmey, P. & Kramer, E.J. 2003. Macromolecules at surfaces: Research challenges and opportunities from tribology to biology. *Journal of Polymer Science Part B: Polymer Physics* 41(22): 2755-2793.

Hennig, G.R. 1959. Interstitial compounds of graphite. *Progress in Inorganic Chemistry* 1: 125-205.

Hou, S., Su, S., Kasner, M.L., Shah, P., Patel, K. & Madarang, C.J. 2010. Formation of highly stable dispersions of silane-functionalized reduced graphene oxide. *Chemical Physics Letters* 501(1): 68-74.

Hummers Jr., W.S. & Offeman, R.E. 1958. Preparation of graphitic oxide. *Journal of the American Chemical Society* 80(6): 1339-1339.

Layek, R.K., Samanta, S. & Nandi, A.K. 2012. Graphene sulphonic acid/chitosan nano biocomposites with tunable mechanical and conductivity properties. *Polymer* 53(11): 2265-2273.

Li, D., Mueller, M.B., Gilje, S., Kaner, R.B. & Wallace, G.G. 2008. Processable aqueous dispersions of graphene nanosheets. *Nature Nanotechnology* 3(2): 101-105.

Morimune, S., Nishino, T. & Goto, T. 2012. Poly(vinyl alcohol)/graphene oxide nanocomposites prepared by a simple eco-process. *Polymer Journal* 44: 1056-1063.

Mukhopadhyay, P. & Gupta, R.K. 2011. Trends and frontiers in graphene-based polymer nanocomposites. *Plastics Engineering* 67: 32-42.

Pan, Yongzheng, Tongfei Wu, Hongqian Bao & Lin Li. 2011. Green fabrication of chitosan films reinforced with parallel aligned graphene oxide. *Carbohydrate Polymers* 83(4): 1908-1915.

Potts, J.R., Dreyer, D.R., Bielawski, C.W. & Ruoff, R.S. 2011. Graphene-based polymer nanocomposites. *Polymer* 52(1): 5-25.

Rana, V.K., Pandey, A.K., Singh, R.P., Kumar, B., Mishra, S. & Ha, C.S. 2010. Enhancement of thermal stability and phase relaxation behavior of chitosan dissolved in aqueous l-lactic acid: Using 'silver nanoparticles' as nano filler. *Macromolecular Research* 18(8): 713-720.

Rhim, J-W., Hong, S-I., Park, H-M. & Ng, K-W. Perry 2006. Preparation and characterization of chitosan-based nanocomposite films with antimicrobial activity. *Journal of Agricultural and Food Chemistry* 54(16): 5814-5822.

Schadler, L.S., Brinson, L.C. & Sawyer, W.G. 2007. Polymer nanocomposites: A small part of the story. *JOM Journal of the Minerals, Metals and Materials Society* 59(3): 53-60.

Shen, J., Li, T., Long, Y., Shi, M., Li, N. & Ye, M. 2012. One-step solid state preparation of reduced graphene oxide. *Carbon* 50(6): 2134-2140.

Stankovich, S., Dikin, D.A., Dommett, G.H.B., Kohlhaas, K.M., Zimney, E.J., Stach, E.A., Piner, R.D., Nguyen, S.B.T. & Ruoff, R.S. 2006. Graphene-based composite materials. *Nature* 442(7100): 282-286.

Szabó, T., Szeri, A. & Dékány, I. 2005. Composite graphitic nanolayers prepared by self-assembly between finely dispersed graphite oxide and a cationic polymer. *Carbon* 43(1): 87-94.

Tang, C., Xiang, L., Su, J., Wang, K., Yang, C., Zhang, Q. & Fu, Q. 2008. Largely improved tensile properties of chitosan film via unique synergistic reinforcing effect of carbon nanotube and clay. *The Journal of Physical Chemistry B* 112(13): 3876-3881.

Veerapandian, M., Lee, M.H., Krishnamoorthy, K. & Yun, K. 2012. Synthesis, characterization and electrochemical properties of functionalized graphene oxide. *Carbon* 50(11): 4228-4238.

Vijay Kumar, S., Huang, N.M., Lim, H.N., Marlinda, A.R., Harrison, I. & Chia, C.H. 2012. One-step size-controlled synthesis of functional graphene oxide/silver nanocomposites at room temperature. *Chemical Engineering Journal* 219: 217-224.

Wang, G., Yang, J., Park, J., Gou, X., Wang, B., Liu, H. & Yao, J. 2008. Facile synthesis and characterization of graphene nanosheets. *The Journal of Physical Chemistry C* 112(22): 8192-8195.

Wang, S.F., Shen, L., Tong, Y.J., Chen, L., Phang, I.Y., Lim, P.Q. & Liu, T.X. 2005. Biopolymer chitosan/montmorillonite nanocomposites: Preparation and characterization. *Polymer Degradation and Stability* 90(1): 123-131.

Yang, X., Tu, Y., Li, L., Shang, S. & Tao, X. 2010. Well-dispersed chitosan/graphene oxide nanocomposites. *ACS Applied Materials & Interfaces* 2(6): 1707-1713.

N.I. Syuhada, N.M. Huang*, S.A. Rahman & G.S. Thien
Low Dimensional Materials Research Centre
Department of Physics
University of Malaya
50603 Kuala Lumpur
Malaysia

S. Vijay Kumar
Laboratoire de Chimie Physique Macromoléculaire
ENSIC, Université de Lorraine
1 rue Grandville, BP 20451
54 001 Nancy Cedex
France

H.N. Lim, N.A. Ibrahim, M. Ahmad & P. Moradihamedani
Department of Chemistry, Faculty of Science
Universiti Putra Malaysia
43400 Serdang, Selangor
Malaysia

*Corresponding author; email: huangnayming@um.edu.my